Article (refereed) - postprint

Gacia, Esperança; Soto, David X.; Roig, Romero; Catalan, Jordi. 2021.
Phragmites australis **as a dual indicator (air and sediment) of trace metal pollution in wetlands – the key case of Flix reservoir (Ebro river)**.

The definitive version was published in *Science of the Total Environment* (2021), 765. 142789. https://doi.org/10.1016/j.scitotenv.2020.142789

The definitive version is available at https://www.elsevier.com/

ms. accepted in *Science of the Total Environment* October 2020

Phragmites australis as a dual indicator (air and sediment) of trace metal pollution in wetlands – the key case of Flix reservoir (Ebro River)

Esperança Gacia*[1], David X. Soto[2], Romero Roig[1], Jordi Catalan[3,4]

[1]Centre d'Estudis Avançats de Blanes, CSIC. Ctra. Accés Cala Sant Francesc 14, 17300 Blanes, Catalonia, Spain.

[2]UK Centre for Ecology and Hydrology, Library Avenue, Lancaster LA1 4AP, UK

[3]CREAF, Edifici C, Campus UAB, E-08193 Cerdanyola del Vallès, Catalonia, Spain.

[4]CSIC, Campus UAB, E-08193 Cerdanyola del Vallès, Catalonia, Spain

Short title: *Phragmites* as a dual indicator of trace metals

19

Abstract

Evaluation of trace metal pollution in an environmentally complex context may require the use of a suite of indicators. Common reed, *Phragmites australis,* is a well-known biomonitor of sediment pollution. Here, we show its potential for also assessing air pollution. The plant panicles, holding silky hairs with high surface to volume ratio, are appropriate collectors of atmospheric contaminants, which perform independently from root bioconcentration. We applied the dual value of common reed as an indicator of trace metal pollution to the case of a chlor-alkali plant in the Ebro river bank (Spain). This factory had historically damped waste to the shallow Flix reservoir. Extensive common reed meadows are growing on the top of the waste, in a nearby nature reserve across the reservoir and a meander immediately downriver. Three replicated individuals from a total of 11 sites were sampled, and the trace metal content measured in the main plant compartments (roots, rhizomes, stems, leaves, and panicles). Panicles and roots showed a much larger concentration of trace metals than the other plant compartments. Levels of Hg, Cu, and Ni were markedly higher in panicles at the factory and nearby points of the reserve and lowered at the meander. In contrast, Cd, Zn, and Mn in roots increased from the factory to the meander downriver. We conclude that panicles show recent (less than a year) airborne pollution, whereas roots indicate the long-term transport of pollutants from the waste in the shoreline of the factory to downriver sedimentation hotspots, where they become more bioavailable than in the factory waste. The Hg spatial patterns in panicles agree with air measurements in later years, therefore, confirming the panicles suitability for assessing airborne pollution and, consequently, *Phragmites* as a potential dual biomonitor of air and sediments.

Keywords: common reed, airborne Hg, panicles, Cd dispersion, roots, metal bioavailability

1. Introduction

The use of selected organisms as biomonitors facilitates the assessment of trace metal pollution, bioavailability, and comparison among sites. The choice of species is crucial for pollution detection and quantification and depends on the question, habitat, and time scales considered (Soto et al. 2011). The evaluation of different pollution sources (e.g., air, water, sediment, suspended material, or other organisms) requires a suite of indicators with complementary properties (Luoma and Rainbow 2008). In wetlands, an organism's exposure to pollutants differ between aerial and aquatic media and, consequently, different biomonitors could be selected. However, helophytes — plants with perennial parts in the mud below the water level, and aerial stems, leaves, and inflorescences — are present in both media. We suggest that this feature can be exploited for dual assessment of air and sediment pollution. In particular, here we introduce the case of the common reed (*Phragmites australis* (Cav.) Trin. Ex Steud): an emergent aquatic plant, which is common in wetlands, the littoral of ponds and lakes, riverbanks, and even marginal wet habitats in urban areas. Common reed shows a worldwide distribution, being native of the Northern Hemisphere has become invasive across all continents. This feature, not particularly satisfactory for biodiversity conservation, becomes an attractive property for environmental bioassessments

The plant shows erect stems, linear leaves, and bushy panicles as inflorescences. Flowering typically occurs in late summer. The plant withstands extreme environmental conditions, including the exposure and accumulation of toxic pollutants such as Cd, Hg, Cu, Mn, Zn, Ni, Cr, Pb and As (Batty and Younger 2004; Bragato et al. 2009; Lominchar et al. 2015); thus it is used for detoxification and stabilization of metal sludge (Bonanno et al. 2017). Common reed metal bioconcentration mainly occurs in the roots (i.e. Weis and Weis 2004; Bonanno 2011). There is abundant literature proving quantitative relations between this plant part and the environment (Eid and Shaltout 2014; Phillips et al. 2015; Eid et al. 2020, among others); consequently, the common reed is a well-accepted trace metal biomonitor of sediment pollution (Bonnano and Lo Giudice 2010; Yuan et al. 2016). Trace metal bioavailability and bioconcentration depend on environmental properties such as temperature, season, salinity, oxygen demand, pH and metal concentration (Bonanno and Lo Giudice, 2010; Vymazal and Brezinova 2016) as well as plant age.

Interestingly, the metal translocation from roots to the other plant parts (i.e., leaves, rhizomes, and stems) is usually low (Bonanno et al. 2017). For this reason, leaves were tentatively proposed as potential indicators of air pollution (Bonanno and Pavone 2015). However, the accumulation in the inflorescences (i.e., panicles) has not been assessed yet, but there is no reason to expect a higher internal transport from roots than to the other parts of the plant. The physical structure of the panicles with flowers surrounded by abundant silky hairs offer much surface for direct trapping of air pollutants. Consequently, we hypothesized that common reed panicles could be useful for monitoring air contamination around industrial areas, performing similarly as mosses and lichens (Calasans and Malm 1997; Lodenius 1998; Fernandez et al. 2000), in which adsorption and absorption may occur.

The aim of this study, therefore, was to test for the potential dual role of *P. australis* as an indicator of airborne and sediment trace metal pollution. For this assessment, we used the case study of a chlor-alkali plant in the Ebro river bank (Spain) with a long history of environmental pollution (Palanques et al. 2014). We measured trace metal concentrations in several parts of the same plant individuals and analyzed the coherence of the patterns observed with the assumption of transport from sediments to roots and from there to other plant compartments but with low transfer ratios. We expected panicles to show discrepancies with this assumption if affected directly by airborne pollution. In this case, panicles should show a trace metal composition different from that in the sediment and roots, and, in our study case, spatial patterns coherent with air pollution transport from a specific point source, the factory.

2. Material and methods

2.1 Study area and sampling

The lower Ebro River basin (Spain) shows a Mediterranean climate with high seasonal variation in precipitation, with dry, hot summers and wet, cold winters. The average annual temperature is 16 °C and rainfall 560 L m^{-2} in the study area. The Flix reservoir (41.23 N; 0.53 E) is small (area: 3.2 km^2, volume: 11 x 10^6 m^3), shallow (maximum depth 10 m), and with a short water residence time (0.3 days; Navarro et al., 2006). Its riverbanks show contrasting characteristics (Fig. 1). The chlor-alkali plant locates on the southern side —right side according to the river flow — and, in front of the factory, there is a large waste area accumulated over 100 years (EU 2007) on top of which common reed was growing. On the northern side, there is a wildlife reserve that includes a large wetland area dominated by common reed. Immediately after the reservoir dam, the river meanders, and a large population of common reed develops there (Fig. 1b). Common reed areal plant biomass at the factory (2.43 ± 0.6 kg DW m^{-2}) did not significantly differ from the reserve (mean 4.59 ± 4.35 kg DW m^{-2}, ANOVA $p > 0.05$). Unfortunately, we do not have biomass data for the meadows at the meander but was similarly high.

A major restoration started in 2012 that removed the highly polluted sludge from the southern reservoir shoreline. Our study was conducted previously to the waste removal and considered the three main common reed areas, namely, the factory waste (F), the reserve (R), and the meander (M). Three (R and M) to five (F) sampling points were selected in each site of an approximate 4 m^2 area (Fig. 2).

In May 2006, three young green individual plants were collected in each sampling point to measure trace metal accumulation in all plant compartments, including panicles from the previous growing season (i.e., late summer-fall 2005) and corresponding to brown, older individuals that have been exposed to airborne pollution for about one year. Samples were collected using gloves, sorted in plant parts, namely, leaf, stems, rhizomes, roots, and panicles, stored in polypropylene plastic bags, and frozen immediately in the field. All parts were wiped, except panicles, because their fragility and aim to measure the entire trace metal content trapped in these hairy structures. At the lab, the samples were freeze-dried before further processing. Some extra samples were collected and dried at 60 °C to assess the aboveground biomass as dry weight.

2.2 Trace metals analysis

Plant material was ground with a mortar (Retsch RM200) before metal extraction. Three replicates of 50-100 mg of each sample powder were acid digested in 60-ml closed Teflon vessels under microwaves and high-pressure (15 min, 200 °C), following the DIN 38414-S7 method. Extracts were diluted with HNO_3 0.5 M to 50 ml and trace metals (Cr, Mn, Fe, Ni, Cu, Zn, As, Se, Cd, Hg, and Pb) analyzed by inductively coupled plasma - mass spectrometry (ICP-MS; Perkin-Elmer Elan-6000). Analytical accuracy was assessed by including three blanks and three samples of reference material (i.e., hay powder - IAEA-V-10) in every extraction and digestion. Recovery efficiency for all metals is shown in Table A.1, although, eventually, results were not corrected by recovery efficiency. Levels of As, Se, and Hg of the reference material were below the detection limit; therefore, we estimate the analytical performance based on the above detection limit replicated samples from the study (Table A.1). All reagents used were Merck Suprapur. Detection limits in the extracts were 5.00 µg L^{-1}, Fe; 1.00 µg L^{-1}, Se; 0.25 µg L^{-1}, Zn and Cr; 0.10 µg L^{-1}, As, Hg and Ni; 0.05 µg L^{-1} Cu, Mn, and Pb; 0.03 µg L^{-1} Cd.

2.3 Numerical methods

We used Statistica for descriptive statistics and Primer-Permanova v6 for principal component analysis (PCA) of the metal composition in the different plant parts. Data were log-transformed and standardized before multivariate analysis. Since metal concentration in plant tissues did not show homoscedasticity, we used Wilcoxon and Kruskal-Wallis to tests for differences. Spearman rank correlation was used to assess the influence of distance to the pollution focus in the metal content in roots and exponential fitting to assess the decay in the metal content of the panicles from the factory downwards.

Bioconcentration factors (BCF) — percentual ratios of each trace metal between roots and sediment —were estimated using sediment data collected in the same study area and time (Bosch et al. 2009). Translocation factors (TF) were calculated as the ratio among plant parts and root trace metal content. We did not measure metal content in wiped panicles; therefore, we cannot estimate TF for panicles, although there is no reason that could be higher than for other plant parts (e.g., leaves).

3. Results

3.1 Trace metal distribution across sites and compartments

The highest Hg levels in each plant compartment were found at the factory site, particularly in the panicles (Fig. 3; Table A.2). Panicles were also highly loaded with Ni, Cu, and Cr at this site (Fig. 3; Table A.2). In contrast, the highest levels of Cd and Zn in roots, and Se in all plant parts were found at the meander (Fig. 3; Table A.2). At the reserve, roots and rhizomes were particularly rich in As (Fig. 3; Table A.2).

The PCA ordination of all common reed metal samples showed the existence of strong gradients in roots and panicles across sites (Fig. A.1). The rest of the plant compartments showed lower variation and were more homogeneous among sites. The first PCA axis ordered the samples following the absolute metal load (PC1 54.5% variance), which was low in all compartments except for roots and panicles, as mentioned above. The second axis (PC2 14% variance) differentiated panicles from roots. The former were rich in Hg, Ni, and Cr, particularly at the factory, while roots showed a more heterogeneous metal content and variation among sites, being notably different those at the reserve rich in As, Fe and Mn (Fig. A.1).

3.2 Translocation factors between compartments

The translocation factors between roots and other compartments were, in general, low, well below 1 (Table A.3). This feature was particularly outstanding in the case of the rhizome, with the only exception for selenium. Indeed, Se showed consistent translocation factors from roots to other compartments around 0.5 or higher. Other trace metals showed less coherent translocation factors between roots and other compartments.

Mn showed translocation factors above one from roots to leaves but below 0.3 to stem and rhizome. The rest of trace metals did not exceed root levels in other compartments in any case, and in general, were rather low (<<0.2) except for Cu and Zn, as expected for micronutrients. The translocation factor of metals between stems to leaves was >1 in most cases (up to 5.4), differentiating the transport nature of stems from that of leaves as final end-points.

3.3 Roots biomonitoring

Concerning roots, there were Hg high levels and broad dispersion at the factory (Fig. 3). Arsenic, in contrast, was much higher at the reserve, although also showing large variation between points and individuals (Fig. 3). The roots in the meander were significantly enriched in Cd and Se, while Fe and Mn were significantly low at the factory (Fig. 3; Table A.2).

The PCA of the root samples (Fig. A.2) showed an increasing gradient in Cd and Pb levels from individuals at the factory to those at the meander (PC1 38.8% variance). Also, a strong gradient of As occurred, with maximum values at the reserve and opposed to Se levels (PC2 25.3% variance). The third axis, not shown, indicated high Hg levels in roots at the factory and some points nearby the reserve and lower at the inner reserve and meander (PC3 12.5% variance).

Some metals were unexpectedly lower in reed roots on the top of the waste than downriver in the meander. The pattern was a linearly increasing tendency with distance, significant for Mn, Cd, and Zn (Table 1) within the study area. Nonetheless, R^2 values were low, because the highest values were found in the first point in the meander (point 9, Fig. 2), just after the reservoir dam and declaimed in the two following sampling points downstream.

The BCFs for Hg were very high in roots at the factory and reserve, the sites closest to the waste (Table 2). Arsenic highly concentrated in the roots of the reserve, concomitant with the high levels in sediment (Table 2). Roots at the meander registered the highest BCF for the other trace elements even though their levels in sediment were less concentrated than at the factory and the reserve (Table 2).

3.4 Panicles as indicators of airborne metal pollution

Mercury levels in panicles differed between the tree sites significantly (Table A.2). There were much higher Hg levels at the factory (Fig. 3) —note the logarithmic scale in the figure— followed by the reserve and low levels at the meander. Cd showed a similar trend but smoother and with only significantly lower values at the meander. In contrast, the meander showed significantly higher levels of Mn and Fe (Table A.3). The rest of trace metals (Se, Cr, Zn, Ni, As, and Pb) showed high variation within sites and non-significant differences among them. The PCA of metals in panicles summarized these patterns (Fig. A.2). The main variation was associated with Hg (PC1 58.4% variance) with higher values at the factory and in one sampling site in the reserve (point 7, Fig. 2). The second axis related to Se, which showed a marked gradient at the meander (PC2 16.6% variance).

Assuming that the factory is the current point source and transport by air diffusion, it could be expected an exponential decline in panicles trace metal content with increasing distance to that point source. Indeed, the levels of Hg, Cu, Ni, and Cd experienced an exponential decline from the closest sampling points to the factory to those far away in the meander (Table 1 and Fig. 4a).

4. Discussion

4.1 Flix hotspot of pollution

In the Flix and meander reservoir system, *Phragmites australis* presented the highest Hg levels in roots - and also high Cr, Cu, Cd and As - compared to other polluted wetlands and phytoremediation areas up to now studied (Weis & Weis 2004; Vymazal and Březinová 2016; Cicero-Fernández and Fernández 2016; 2017). These results confirm that Flix was a Hg hotspot of pollution in Spain and other aquatic areas of the EU (Esbri et al. 2015) and strongly support the decision to remove the toxic waste from the reservoir - which has brought to one of the major operations of environmental and ecological restoration in Europe (EU, 2007) - and also to stop the activity of the old chlor-alkali plant in 2020.

4.2 Downriver transport and bioavailability

The spatial pattern of trace metal content in plant roots was complex. At the factory, Hg reached the highest levels consistent with the too high concentration found in the waste upper layer (Bosch et al. 2009). Differently, Cd, Se, Zn, and Cu in roots reached its maximum at the meander, despite being extremely concentrated at sub-superficial layers of the factory deposits (Palanques et al. 2014). This is coherent with previous studies indicating erosion and downstream transport of polluted sediments and further accumulation of suspended material in the depositional areas of the meander (Tena and Batalla 2013; Palanques et al. 2019), and with the different biogeochemical conditions in both areas.

At the factory, the wastes were extremely oxidant because they contained NaClO (Palanques et al. 2014), which prevented vertical metal mobility but not the most recent accumulation of Hg in the upper sediment layer. At the meander, the conditions of high oxygen demand in wetland sediments, particularly in this slow flow area, and the enrichment in the organic component of the sediment (Bosch et al. 2009) likely favored trace metal mobility and bioavailability to roots. This view is supported by the highest bioaccumulation of all trace metals in this meander zone, except Hg, even though the levels in sediments were lower than at the factory. More specifically, the existence of high levels of Mn may displace Cd bound to organic matter and fine sediments

(Argüello et al. 2019), thus promoting the bioavailability of Cd as seen for the high levels in roots, and toxicity assays (see Bosch et al. 2009). Interestingly, although downriver transport of Hg in sediment particles has been reported (Carrasco et al. 2008; Tena and Batalla 2013; Palanques et al. 2019), the Hg levels were relatively low in the roots at the meander and inversely related to high Se levels, which acts antagonistically, declining Hg bioavailability as well as organic matter (Dang et al. 2019).

At the wildlife reserve, roots showed high As which is coherent with baseline levels in the Ebro catchment (Carbonell unpublished results) and local conditions for high bioavailability when iron is abundant (Bidone et al. 2018). The BCFs from sediment to roots were large, more than 50%, but the TF from the roots to the other plant compartments were lower than one. Only leaves tended to accumulate As from stems. The relatively low Cd and other trace metals in *P. australis* roots at the reserve indicates that the river flow prevents metal transport across the reservoir, washing out suspended material and pollutants downriver.

4.3 Trace metal bioconcentration

Despite the high concentrations of trace metals recorded in the sediment and roots of *P. australis* at Flix, the BCFs were of the same order or even lower than in other localities. Specifically, there was a relatively low bioavailability of metals such as Hg, Cr, Ni, and As in Flix compared to coastal wetlands (Bonnano et al. 2018). Adaptations for salt tolerance in varieties inhabiting coastal zones, which may interfere with metal toxicity, may be the explanation (Anjun et al. 2014).

Multifactorial mechanisms determine trace metal bioavailability to roots in wetland plants. *P. australis* was found to bioconcentrate the most among many other wetland species in a coastal lagoon (Bonnano et al. 2018), but in other systems, e.g., lake Burrus, bioaccumulation of Cd, Zn, Cu and Ni in *Typha dominguensis* (Eid et al. 2020b) was more substantial. The estimated transfer of metals from roots to the other plant compartments at Flix was also in general much lower than in *P. australis* from coastal lagoons suggesting that marine influence (i.e., salinity) promotes the transfer of Hg, Cd, Cr, Pb and As from roots to leaves in common reed as described for Cu, Zn and Cr in intertidal marshes (Du Laing et al. 2009). Transfer of Mn, Zn, Cu, and Ni remained at similar levels at Flix than in the coastal wetland study of (Bonnano et al. 2018). Accordingly, trace metals in common reed would be less transferred to aerial food webs (e.g., by bird seed-feeding) in freshwaters, such as in Flix, than in coastal marshes provided that biomass per unit area is similar. Our results confirm the complex and often weak relationship between root metal content and overall plant bioaccumulation (Vymazal and Březinová 2016). The complexity and variability of trace metal bioaccumulation in common reed modify its potential for sediment bioremediation depending on the environmental conditions. As a biomonitor of trace metal in sediments, our results suggest a need for distinguishing between salty and freshwater environments in case of global comparisons.

4.4 Common reed as a dual indicator

The potential of *P. australis* as a dual indicator of sediment and airborne pollution is evidenced by the sharp contrast in metal content between plant roots and panicles across the three study sites. The other plant compartments (i.e., leaves, stems, and rhizomes) showed a relatively homogenous and low trace metal content, in agreement with a low transfer of metals from roots to the other plant parts, which is interpreted as a mechanism to prevent toxicity (Weis and Weis 2004; Bonanno 2011; Phillips et al. 2015).

In panicles, the content of Hg, Cu, Ni, and Cd experienced an exponential decline at increasing distance from the chlor-alkali plant, with extremely high concentrations at the points closer to the factory chimney — which included points at the reserve— and low values at the meander; thus clearly showing the accumulation of recently airborne contaminants from the factory in this hairy plant compartment. In this rural area, there is no other source point of atmospheric mercury that could provide an alternative explanation. In the following year to our study and for five years, López Berdonces et al (2017) measured air Hg around the factory. The air Hg spatial pattern that they found was very consistent with our measurements in panicles (Fig. 4). Furthermore, the levels encountered in the thalli of the lichen *Xanthoria parietina*, between the years 2007 to 2012 in the same study, showed the same range that our panicles' data, sampled just a year before. Hg in *Xanthoria* correlated to air Hg significantly. Therefore, panicles of *P. australis* appear to be as good as lichens to assess Hg contamination, with the advantage of being much more abundant in wetland areas. Beyond Hg, panicles also showed that Cu, Ni, and Cd experienced aerial dispersion similar to Hg in the studied area, which were not measured in López Berdonces et al (2017).

On the view of these results, we propose *P. australis* panicles as a potential new system for the biomonitoring of airborne pollution useful for periods from months to a year, which corresponds to the growing period and presence (even when dry) of the reproductive organs of *P. australis*. The panicle temporal exposure can be approximately assessed using the changes in color through its development; that is, pale green (days), purple (weeks), and brown (months). Although slow-growing lichens or mosses are commonly used for air trace metal biomonitoring, their presence may be restricted in certain landscapes (e.g., Mediterranean wetlands) and present limitations for encountering the same species over distant locations and large regions (Szczepaniak and Biziuk 2003). The widespread common reed might provide a useful complementary system to include in the toolbox for biomonitoring air pollution.

In our case study, the dual indicator capacity of *P. australis* has allowed disentangling a complex mosaic of industrial pollution resulting from the combination of heavily polluted waste and sediments accumulated at the Flix reservoir throughout many years and the ongoing air emissions of the chlor-alkali plant. The airborne pollution affects the areas closest to the focus at the southern side of the river bank and also across the river at the natural reserve where autochthonous horses are raised. Interestingly, this pollution pattern is different from the one detected by roots in the sediments, in which the meander is a hotspot of several toxic metals as a result of upstream waste erosion plus sediment conditions enhancing their bioavailability.

4.5 Concluding remarks

Altogether our results show that the use of the cosmopolitan wetland plant species *Phragmites australis* can be an excellent tool for assessing airborne and sediment trace metal pollution. We suggest its use in the Flix area after finishing the ongoing environmental restoration. Nonetheless, further work is needed across different sites to definitively establish and quantitatively calibrate the common reed panicles as air biomonitor. Significantly, better knowledge of the mechanisms of bioaccumulation adsorption and absorption and variation with the panicle aging and environmental circumstances will facilitate their optimal application and, also, its performance comparison with other air biomonitors (e.g., lichens, mosses, trees). Common reed panicles are likely to offer complementary options rather than competing alternatives. Aside from its role in biomonitoring, common reed panicles are a source of food for part of the rich fauna in wetlands (e.g., birds and insects). Therefore, it has to be considered as a potential source of trace metal contamination for those organisms, another line of further investigation.

Acknowledgements

Financial support was provided by the MOBITROF project (Spanish Ministry of the Environment and Rural and Marine Affairs and the Catalan Agency of Water), GRACCIE project (CSD2007-00067), ECO_Reactor PN I+D+I MINECO ref. PGC2018-101975-B-22. 2019-2022, and Grup de Recerca de Canvis Ambientals GECA (SGR-DGR), Generalitat de Catalunya, 2017SGR-910 (36-674), 2018-2021. D.X. Soto acknowledges an FPU fellowship from the Spanish Ministry of Education.

Literature references

Anjum, N.A., Ahmad, I., Válega, M., Mohmood, I., Gill, S.S., Tuteja, N., Duarte, A.C., Pereira, E., 2014. Salt marsh halophyte services to metal-metalloid remediation: Assessment of the processes and underlying mechanisms. Crit. Rev. Environ. Sci. Technol. 44, 2038–2106. https://doi.org/10.1080/10643389.2013.828271

Argüello, D., Chavez, E., Lauryssen, F., Vanderschueren, R., Smolders, E., Montalvo D., 2019. Soil properties and agronomic factors affecting cadmium concentrations in cacao beans: A nationwide survey in Ecuador. Sci. Total Environ. 649, 120-127. https://doi.org/10.1016/j_scitotenv2018.08.292

Batty, L.C., Younger, P.L., 2004. Growth of *Phragmites australis* (Cav.) Trin ex. Steudel in mine water treatment wetlands: Effects of metal and nutrient uptake. Environ. Pollut. 132, 85–93. https://doi.org/10.1016/j.envpol.2004.03.022

Bidone, E., Cesar, R., Santos, M.C., Sierpe, R., Silva-Filho, E.V., Kutter, V., Dias da Silva, L.I., Castilhos, Z., 2018. Mass balance of arsenic fluxes in rivers impacted by gold mining activities in Paracatu (Minas Gerais State, Brazil). Environ. Sci. Pollut. Res. 25, 9085–9100. https://doi.org/10.1007/s11356-018-1215-z

Bonanno, G., 2011. Trace element accumulation and distribution in the organs of *Phragmites australis* (common reed) and biomonitoring applications. Ecotoxicol. Environ. Saf. 74, 1057–1064. https://doi.org/10.1016/j.ecoenv.2011.01.018

Bonanno, G., 2013. Comparative performance of trace element bioaccumulation and biomonitoring in the plant species *Typha domingensis*, *Phragmites australis* and *Arundo donax*. Ecotoxicol. Environ. Saf. 97, 124–130. https://doi.org/10.1016/j.ecoenv.2013.07.017

Bonanno, G., Borg, J.A., Di Martino, V., 2017. Levels of heavy metals in wetland and marine vascular plants and their biomonitoring potential: A comparative assessment. Sci. Total Environ. 576, 796–806. https://doi.org/10.1016/j.scitotenv.2016.10.171

Bonanno, G., Lo Giudice, R., 2010. Heavy metal bioaccumulation by the organs of *Phragmites australis* (common reed) and their potential use as contamination indicators. Ecol. Indic. 10, 639–645. https://doi.org/10.1016/j.ecolind.2009.11.002

Bonanno, G., Pavone, P. (2015). Leaves of *Phragmites australis* as potential atmospheric biomonitors of Platinum Group Elements. Ecotox Environ Safe, 114, 31–37. doi:https://doi.org/10.1016/j.ecoenv.2015.01.005

Bonanno, G., Vymazal, J., Cirelli, G.L., 2018. Translocation, accumulation and bioindication of trace elements in wetland plants. Sci. Total Environ. 631–632, 252–261. https://doi.org/10.1016/j.scitotenv.2018.03.039

Bosch, C., Olivares, A., Faria, M., Navas, J.M., del Olmo, I., Grimalt, J.O., Piña, B., Barata, C., 2009. Identification of water soluble and particle bound compounds causing sublethal toxic effects. A field study on sediments affected by a chlor-alkali industry. Aquat. Toxicol. 94, 16–27. https://doi.org/10.1016/j.aquatox.2009.05.011

Bragato, C., Schiavon, M., Polese, R., Ertani, A., Pittarello, M., Malagoli, M., 2009. Seasonal variations of Cu, Zn, Ni and Cr concentration in *Phragmites australis* (Cav.) Trin ex steudel in a constructed wetland of North Italy, Desalination.

Calasans, C.F., Malm, O., 1997. Elemental mercury contamination survey in a chlor-alkali plant by the use of transplanted Spanish moss, *Tillandsia usneoides* (L.). Sci. Total Environ. 208, 165–177. https://doi.org/10.1016/S0048-9697(97)00281-7

Carrasco, L., Díez, S., Soto, D.X., Catalan, J., Bayona, J.M., 2008. Assessment of mercury and methylmercury pollution with zebra mussel (*Dreissena polymorpha*) in the Ebro River (NE

Spain) impacted by industrial hazardous dumps. Sci. Total Environ. 407, 178–184. https://doi.org/10.1016/j.scitotenv.2008.07.031

Cicero-Fernández, D., Peña-Fernández, M., Expósito-Camargo, J.A., Antizar-Ladislao, B., 2017. Long-term (two annual cycles) phytoremediation of heavy metal-contaminated estuarine sediments by *Phragmites australis*. N. Biotechnol. 38, 56–64. https://doi.org/10.1016/j.nbt.2016.07.011

Cicero-Fernández, D., Peña-Fernández, M., Expósito-Camargo, J.A., Antizar-Ladislao, B., 2016. Role of *Phragmites australis* (common reed) for heavy metals phytoremediation of estuarine sediments. Int. J. Phytoremediation 18, 575–582. https://doi.org/10.1080/15226514.2015.1086306

Dang, F., Li, Z., Zhong, H., 2019. Methylmercury and selenium interactions: Mechanisms and implications for soil remediation. Crit. Rev. Environ. Sci. Technol. 49, 1737-1768. https://doi.org/10.1080/10643389.2019.1583051

Du Laing, G., Van de Moortel, A.M.K., Moors, W., De Grauwe, P., Meers, E., Tack, F.M.G., Verloo, M.G., 2009. Factors affecting metal concentrations in reed plants (*Phragmites australis*) of intertidal marshes in the Scheldt estuary. Ecol. Eng. 35, 310–318. https://doi.org/10.1016/j.ecoleng.2008.01.002

Eid, E.M., Galal, T.M., Shaltout, K.H., El-Sheikh, M.A., Asaeda, T., Alatar, A.A., Alfarhan, A.H., Alharthi, A., Alshehri, A.M.A., Picó, Y., Barcelo, D., 2020b. Biomonitoring potential of the native aquatic plant *Typha domingensis* by predicting trace metals accumulation in the Egyptian Lake Burullus. Sci. Total Environ. 714, 136603. https://doi.org/10.1016/j.scitotenv.2020.136603

Eid, E.M., Shaltout, K.H., 2014. Monthly variations of trace elements accumulation and distribution in above- and below-ground biomass of *Phragmites australis* (Cav.) Trin. ex

Steudel in Lake Burullus (Egypt): A biomonitoring application. Ecol. Eng. 73, 17–25. https://doi.org/10.1016/j.ecoleng.2014.09.006

Eid, E.M., Shaltout, K.H., Al-Sodany, Y.M., Haroun, S.A., Galal, T.M., Ayed, H., Khedher, K.M., Jensen, K., 2020a. Common reed (*Phragmites australis* (Cav.) Trin. ex Steudel) as a candidate for predicting heavy metal contamination in Lake Burullus, Egypt: A biomonitoring approach. Ecol. Eng. 148, 105787. https://doi.org/10.1016/j.ecoleng.2020.105787

Esbrí, J.M., López-Berdonces, M.A., Fernández-Calderón, S., Higueras, P., Díez, S., 2015. Atmospheric mercury pollution around a chlor-alkali plant in Flix (NE Spain): an integrated analysis. Environ. Sci. Pollut. Res. 22, 4842–4850. https://doi.org/10.1007/s11356-014-3305-x

EU. Elimination of chemical contamination of Flix reservoir. EU's Cohesion Fund (2007 to 2013). 2010ES161PR001 (2007). http://ec.europa.eu/regional_policy/en/projects/spain/reservoir-clean-up-in-tarragona

Fernández, J.A., Aboal, J.R., Carballeira, A., 2000. Use of native and transplanted mosses as complementary techniques for biomonitoring mercury around an industrial facility. Sci. Total Environ. 256, 151–161. https://doi.org/10.1016/S0048-9697(00)00478-2

Lodenius, M., 1998. Dry and wet deposition of mercury near a chlor-alkali plant. Sci. Total Environ. 213, 53–56. https://doi.org/10.1016/S0048-9697(98)00073-4

Lominchar, M.A., Sierra, M.J., Millán, R., 2015. Accumulation of mercury in *Typha domingensis* under field conditions. Chemosphere 119, 994–999. https://doi.org/10.1016/j.chemosphere.2014.08.085

López Berdonces, M.A., Higueras, P.L., Fernández-Pascual, M., Borreguero, A.M., Carmona, M., 2017. The role of native lichens in the biomonitoring of gaseous mercury at contaminated sites. J. Environ. Manage. 186, 207–213. https://doi.org/10.1016/j.jenvman.2016.04.047

Luoma, S.N., Rainbow, P.S. 2008. Metal contamination in aquatic environments. Cambridge University Press, Cambridge, UK). https://doi.org/10.1111/j.1095-8649.2009.02440_4.x

Navarro, E., Bacardit, M., Caputo, L., Palau, T., Armengol, J. 2006. Limnological characterization and flow patterns of a three-coupled reservoir system and their influence on Dreissena polymorpha populations and settlement during the stratification period. Lake and Reserv. Manag. 22, 293-302. DOI: 10.1080/07438140609354363

Palanques, A., Grimalt, J., Belzunces, M., Estrada, F., Puig, P., Guillén, J., 2014. Massive accumulation of highly polluted sedimentary deposits by river damming. Sci. Total Environ. 497–498, 369–381. https://doi.org/10.1016/j.scitotenv.2014.07.091

Palanques, A., Guillén, J., Puig, P., Grimalt, J., 2019. Effects of flushing flows on the transport of mercury-polluted particulate matter from the Flix Reservoir to the Ebro Estuary. J. Env. Man. 260, https://doi.org/10.1016/j.jenman.2019.110028

Phillips, D.P., Human, L.R.D., Adams, J.B., 2015. Wetland plants as indicators of heavy metal contamination. Mar. Pollut. Bull. 92, 227–232. https://doi.org/10.1016/j.marpolbul.2014.12.038

Soto, D.X., Roig, R., Gacia, E., Catalan, J., 2011. Differential accumulation of mercury and other trace metals in the food web components of a reservoir impacted by a chlor-alkali plant (Flix, Ebro River, Spain): Implications for biomonitoring. Environ. Pollut. 159, 1481–1489. https://doi.org/10.1016/j.envpol.2011.03.017

Szczepaniak, K., Biziuk, M., 2003. Aspects of the biomonitoring studies using mosses and lichens as indicators of metal pollution. Environ. Res. 93, 221–230. https://doi.org/10.1016/S0013-9351(03)00141-5

Tena, A., Batalla, R.J., 2013. The sediment budget of a large river regulated by dams (The lower River Ebro, NE Spain). J. Soils Sediments 13, 966–980. https://doi.org/10.1007/s11368-013-0681-7

Vymazal, J., Švehla, J., Kröpfelová, L., Chrastný, V., 2007. Trace metals in *Phragmites australis* and *Phalaris arundinacea* growing in constructed and natural wetlands. Sci. Total Environ. 380, 154–162. https://doi.org/10.1016/j.scitotenv.2007.01.057

Vymazal, J., Březinová, T., 2016. Accumulation of heavy metals in aboveground biomass of *Phragmites australis* in horizontal flow constructed wetlands for wastewater treatment: A review. Chem. Engin. Journ. 290: 232-242. https://doi.org/10.1016/j.cej.2015.12.108

Yuan, Y., Yu, S., Bañuelos, G.S., He, Y., 2016. Accumulation of Cr, Cd, Pb, Cu, and Zn by plants in tanning sludge storage sites: opportunities for contamination bioindication and phytoremediation. Environ. Sci. Pollut. Res. 23, 22477–22487. https://doi.org/10.1007/s11356-016-7469-4

Weis, J.S., Weis, P., 2004. Metal uptake, transport and release by wetland plants: Implications for phytoremediation and restoration. Environ. Int. https://doi.org/10.1016/j.envint.2003.11.002

Table 1: Functions for the concentration of trace metals in roots (a) and panicles (b) of P. australis at a distance (x) from the focus of contamination: the toxic waste at the factory reservoir site (a) and the factory chimney of the chlor-alkali plant (b). Metal concentration in mg kg-1 DW and distance in m.

a) Metals in roots	R^2	F	p
[Mn] = 95.99 + 0.043 x	0.353	14.77	< 0.001
[Cd] = 0.228 + 0.0003 x	0.224	7.81	< 0.01
[Zn] = 38.57 + 0.0075 x	0.181	5.98	< 0.05

b) Metals in panicles	R^2	F	p
[Hg] = 1.058 $e^{-0.0001x}$	0.732	73.95	< 0.0000
[Cu] = 14.06 $e^{-0.0005x}$	0.502	27.28	< 0.0000
[Cd] = 0.319 $e^{-0.0008x}$	0.326	14.03	< 0.001
[Ni] = 13.65 $e^{-0.0003x}$	0.206	7.025	< 0.02

Table 2: Bioconcentration factors (BCF) for *Phragmites australis* roots.

Metals in sediments (mg Kg FW^{-1})

		Cr	Ni	Cu	Zn	As	Cd	Hg
Upstream	S1	118	320	34	124	17	0.40	0.50
Factory	S2	178	63	41	125	20	0.90	3.00
Near Dam	S3	306	94	47	127	23	1.40	15.10
Meander	S4	34	23	16	61	8	0.60	2.80

Metals in roots (mg Kg FW^{-1})

		Cr	Ni	Cu	Zn	As	Cd	Hg
Reserve	S1	2.25	2.27	3.57	27.86	9.56	0.06	0.15
Factory	S2	1.29	1.78	2.70	27.73	1.98	0.12	1.73
Near Dam	S3	2.34	3.37	2.26	20.76	1.54	0.21	0.13
Meander	S4	2.84	3.18	4.56	41.28	3.27	0.93	0.15

BCF (%)

		Cr	Ni	Cu	Zn	As	Cd	Hg
Reserve	S1	1.9	0.7	10.5	22.5	56.3	15.8	29.6
Factory	S2	0.7	2.8	6.6	22.2	9.9	13.3	57.5
Near Dam	S3	0.8	3.6	4.8	16.3	6.7	14.9	0.8
Meander	S4	8.4	13.8	28.5	67.7	40.9	155.2	5.4

Trace metal concentrations in sediments from Bosch *et al*. (2009) were used in the BCF estimation. Correspondence between sediment and rood data was established as follows: Bosch *et al*.'s Station S1 was used for reserve samples; for the factory, two areas were considered (Station S2 for sampling points 1, 2, and station S3 for points 4 and 5); station S4 for the meander. Trace metal content in roots was averaged accordingly, and the bioconcentration factors calculated as BCF = $[Metal]_{root}/[Metal]_{sediment}$ * 100.

Figure 1. North (a) and South (b) shores of the Flix reservoir in May 2006, at the time when the sampling took place, before the restoration operation.

Figure 2. Air view of the study area in 2006 and the sampling points corresponding to the three sites, namely: Factory (points 1 to 5), Sebes Natural Reserve (points 6, 7, 8), and Meander (points 9, 10, 11).

Figure 3. Trace metal (Hg, Se, Cd, Zn, Cr, Cu, Ni and As) variation in *Phragmites australis* plant compartments (P= panicles, L= leaves, S= stems, Rh= rhizomes, R= roots) among sites (Factory = dark grey, Meander = light grey, and Reserve = white). Boxplots with boxes encompassing 25 and 75% percentiles, and showing the median; whiskers indicate 5 and 95% percentiles. Upper characters indicate sites that are significantly different at $p>0.01$. Metal concentrations are in mg kg^{-1} DW.

Figure 4. Total mercury concentration in common reed panicles (a) and air (b) according to the distance to the chlor-alkali plant in the Flix area. Atmospheric data were extracted from López-Berdonces et al. (2017).

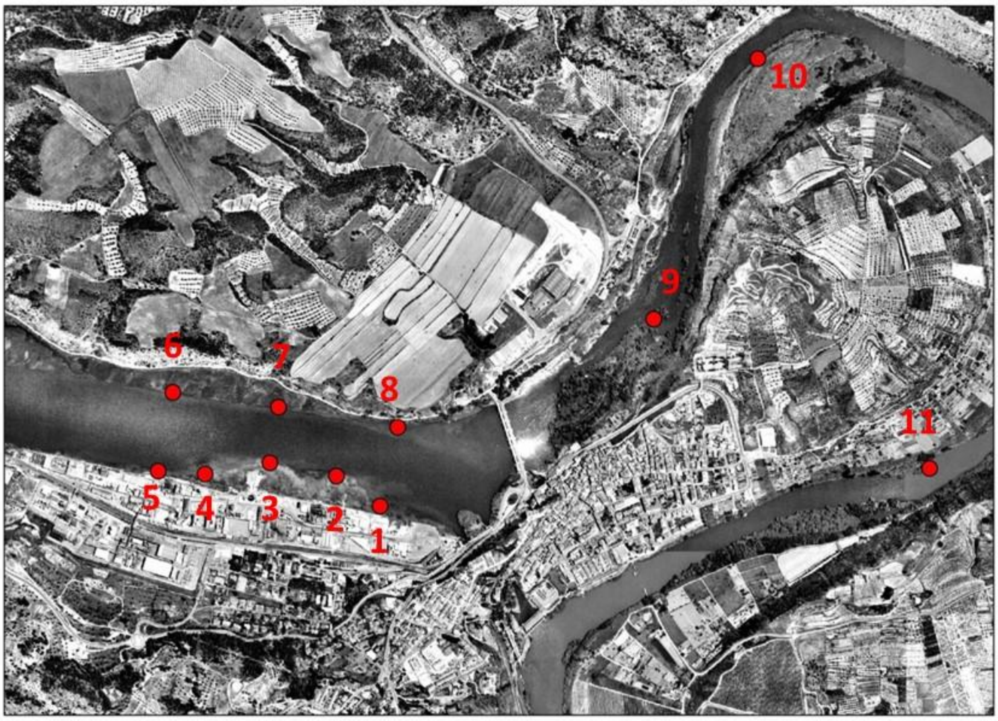
10
9
6
7
8
11
5
4
3
2
1

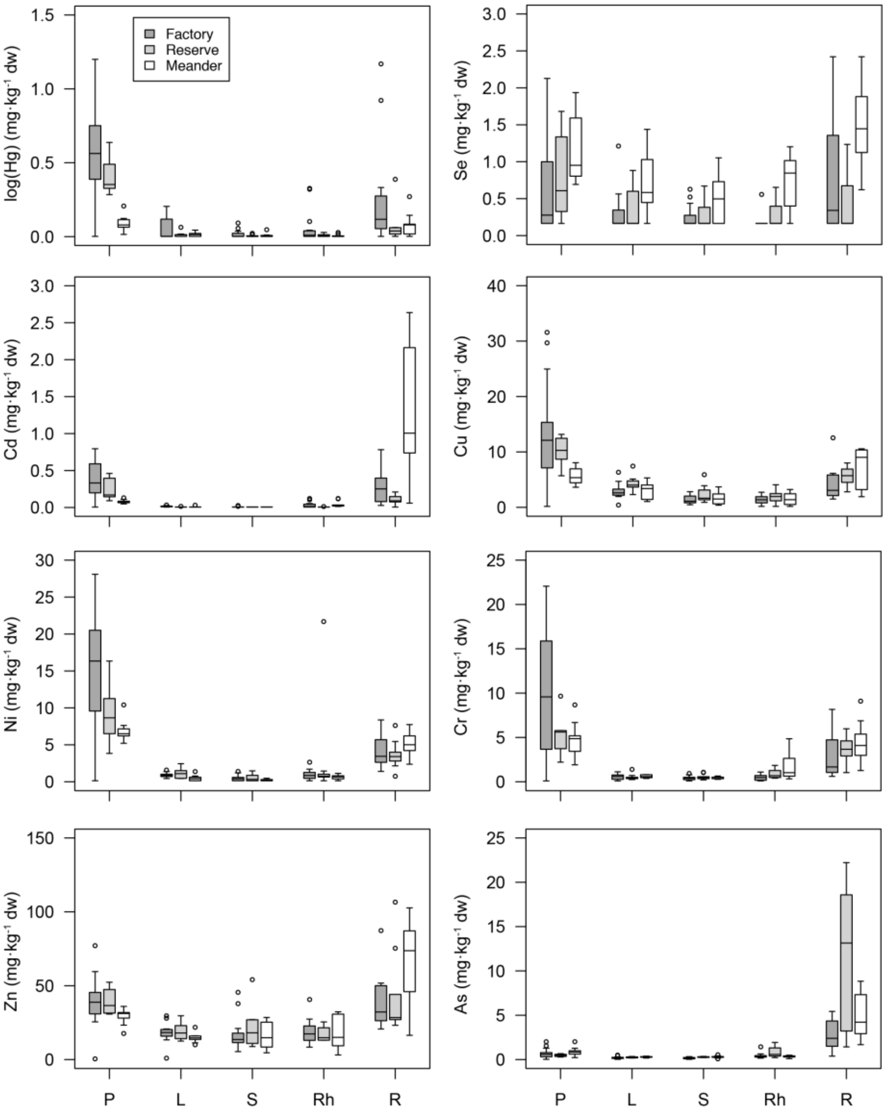
Factory
Reserve
Meander
log(Hg) (mg·kg⁻¹ dw)
Se (mg·kg⁻¹ dw)
Cd (mg·kg⁻¹ dw)
Cu (mg·kg⁻¹ dw)
Ni (mg·kg⁻¹ dw)
Cr (mg·kg⁻¹ dw)
Zn (mg·kg⁻¹ dw)
As (mg·kg⁻¹ dw)
P
L
S
Rh
R

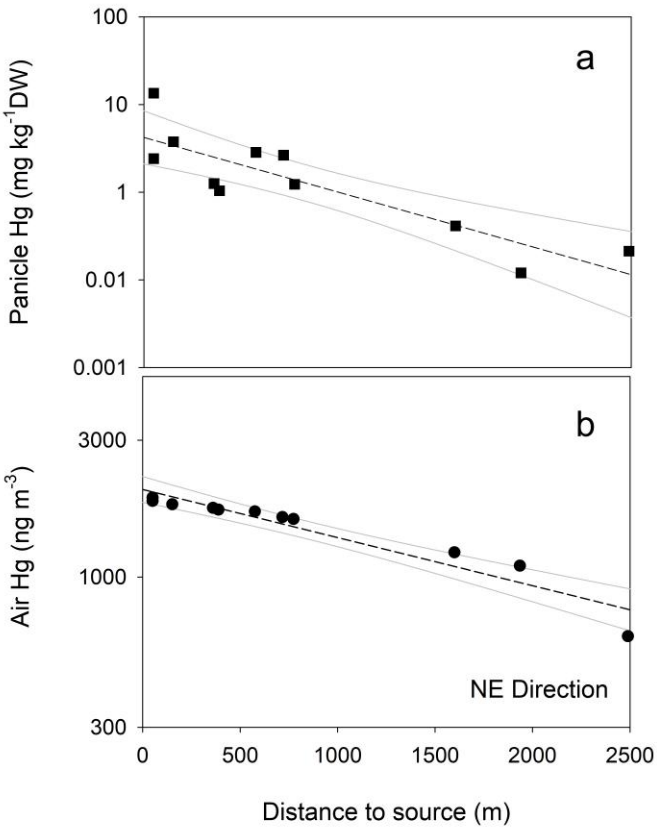
100
10
1
0.01
0.001
Panicle Hg (mg kg-1 DW)
a
3000
1000
300
Air Hg (ng m-3)
b
NE Direction
0
500
1000
1500
2000
2500
Distance to source (m)

503

SUPPLEMENTARY MATERIAL

Phragmites australis as a dual indicator (air and sediment) of trace metal pollution in wetlands – the key case of Flix reservoir (Ebro River)

Esperança Gacia*[1], David X. Soto[2], Romero Roig[1], Jordi Catalan[3,4]

[1]Centre d'Estudis Avançats de Blanes, CSIC. Ctra. Accés Cala Sant Francesc 14, 17300 Blanes, Catalonia, Spain.

[2]UK Centre for Ecology and Hydrology, Library Avenue, Lancaster LA1 4AP, UK

[3]CREAF, Edifici C, Campus UAB, E-08193 Cerdanyola del Vallès, Catalonia, Spain.

[4]CSIC, Campus UAB, E-08193 Cerdanyola del Vallès, Catalonia, Spain

Table A.1. Average recovery efficiency (%) and coefficient of variation (CV) based on three reference samples per digestion and eight digestion runs. Levels of As, Se, and Hg of the reference material were below the detection limit (b.d.), and we estimated a pseudo CV* based on the sample replicates above the detection limit.

	Se	Mn	Zn	Cu	Ni	Cd	Hg	As	Cr	Pb	Fe
Recovery (%)	b.d.	88.5	92.9	88.7	71.4	92.1	b.d.	b.d.	92.7	88.1	90.2
CV	0.18*	0.03	0.04	0.03	0.06	0.08	0.07*	0.06*	0.05	0.05	0.05

Table A.2: Mean and standard deviation (sd) of the trace metal content in plant compartments (PC) of *Phragmites australis* from the three study sites: Factory (F), Reserve (R), and Meander (M). Data are in mg kg^{-1} DW. Varying superscripts indicate significant differences among sites after Kruskal Wallis test and Wilcoxon comparisons per plant compartment.

PC	Site	Hg		Se		Cd		Zn		Cu		Ni		As		Cr		Pb		Mn		Fe	
		mean	sd	mean	sd	mean	sd	mean	sd	mean	sd	mean	sd	mean	sd	mean	sd	mean	sd	mean	sd	mean	sd
Leaves	F	0.16	0.21	0.31	0.16	0.02^{a}	0.01	18.16	5.16	2.91	0.66	0.90^{a}	0.30	0.21	0.08	0.55	0.32	0.16	0.17	127.67	67.15	77.5^{a}	28.8
	R	0.03	0.04	0.34	0.31	0.01^{b}	0.00	19.37	6.17	4.30	0.86	1.08^{a}	0.55	0.26	0.04	0.50	0.22	0.10	0.05	180.00	146.67	77.6^{ab}	80.5
	M	0.03	0.03	0.71	0.15	0.01^{b}	0.00	14.78	3.05	3.02	1.75	0.48^{b}	0.15	0.28^{a}	0.02	0.64	0.15	0.11	0.06	149.35	27.62	93.9^{b}	84.3
Stems	F	0.08	0.11	0.29	0.12	0.01	0.01	19.14	13.37	1.09	0.48	0.58	0.28	0.16^{a}	0.06	0.45	0.27	0.09	0.08	33.16	23.96	30.3^{a}	19.6
	R	0.02	0.02	0.41	0.21	0.01	0.00	17.40	9.90	1.52	0.66	0.45	0.09	0.25^{b}	0.07	0.47	0.12	0.05	0.03	33.10	28.23	30.1^{ab}	15.1
	M	0.01	0.01	0.51	0.15	0.01	0.00	10.74	6.21	1.26	0.69	0.20	0.05	0.19^{b}	0.06	0.39	0.05	0.03	0.00	34.17	3.54	59.4^{b}	42.4
Rhizomes	F	0.19	0.32	0.19^{a}	0.06	0.03^{a}	0.03	18.80	5.82	1.46	0.73	0.94	0.67	0.42	0.18	0.48	0.28	0.12	0.12	28.36^{a}	12.21	53.6^{a}	25.0
	R	0.02	0.02	0.29^{ab}	0.21	0.01^{b}	0.00	17.93	2.38	1.95	0.89	0.71	0.06	0.83	0.70	0.91	0.30	0.09	0.05	29.01^{ab}	20.31	576.3^{b}	746.8
	M	0.02	0.02	0.68^{b}	0.27	0.04^{a}	0.04	16.89	13.40	1.59	1.14	0.62	0.31	0.34	0.09	1.81	1.32	0.09	0.09	35.29^{b}	12.13	106.5^{ab}	61.6
Roots	F	1.74	3.19	0.65^{ab}	0.58	0.25^{a}	0.16	39.91	12.29	4.04	2.06	3.86	2.08	2.89	1.45	2.74	1.73	2.18	2.14	93.46^{a}	58.77	914.8^{a}	416.7
	R	0.24	0.28	0.45^{a}	0.49	0.10^{a}	0.02	44.58	26.88	5.71	1.29	3.63	0.30	15.30	9.26	3.60	0.99	6.19	6.35	154.82^{ab}	104.19	5382.4^{b}	1787.7
	M	0.24	0.23	1.50^{b}	0.14	1.49^{b}	1.14	65.05	27.60	7.29	4.26	5.09	1.92	5.23	2.14	4.55	2.08	5.44	4.36	224.53^{b}	96.77	2771.6^{bc}	915.0
Panicles	F	4.82^{a}	4.95	0.75	0.33	0.45^{a}	0.20	42.96	7.09	15.06^{a}	7.95	18.98	6.91	0.79	0.48	12.46	6.82	2.85	1.33	30.59^{a}	39.78	740.9^{a}	463.8
	R	1.57^{a}	0.75	0.75	0.61	0.30^{a}	0.17	42.43	10.53	10.22^{a}	0.81	9.14	3.48	0.50	0.09	5.34	0.81	2.26	0.31	28.54^{a}	9.58	549.2^{a}	103.3
	M	0.25^{b}	0.15	1.18	0.44	0.08^{b}	0.03	29.11	4.38	5.58^{b}	1.28	6.89	0.98	0.89	0.46	4.71	1.84	2.22	0.66	127.80^{b}	81.26	1906.9^{b}	653.8

Table A.3: *Phragmites australis* transfer factors (TF) among plant compartments for the trace metals measured at the three sampling areas (F= Factory, R= Reserve, and M= Meander).

	TF	Hg	Se	Cd	Zn	Cu	Ni	As	Cr	Pb	Mn	Fe
Leaf/root	F	0.09	0.48	0.08	0.46	0.72	0.23	0.07	0.20	0.07	1.37	0.08
Leaf/root	R	0.13	0.76	0.10	0.43	0.75	0.30	0.02	0.14	0.02	1.16	0.02
Leaf/root	M	0.13	0.47	0.01	0.23	0.41	0.09	0.05	0.14	0.02	0.67	0.05
	average	0.11	0.57	0.06	0.37	0.63	0.21	0.05	0.16	0.04	1.06	0.05
Stem/root	F	0.05	0.45	0.04	0.48	0.27	0.15	0.06	0.16	0.04	0.35	0.03
Stem/root	R	0.08	0.91	0.10	0.39	0.27	0.12	0.02	0.13	0.01	0.21	0.01
Stem/root	M	0.04	0.34	0.01	0.17	0.17	0.04	0.04	0.09	0.01	0.15	0.02
	average	0.06	0.57	0.05	0.34	0.24	0.10	0.04	0.13	0.02	0.24	0.02
Leaf/Stem	F	2.00	1.07	2.00	0.95	2.67	1.55	1.31	1.22	1.78	3.85	2.56
Leaf/Stem	R	1.50	0.83	1.00	1.11	2.83	2.40	1.04	1.06	2.00	5.44	3.15
Leaf/Stem	M	3.00	1.39	1.00	1.38	2.40	2.40	1.47	1.64	3.67	4.37	2.27
	average	2.17	1.10	1.33	1.15	2.63	2.12	1.28	1.31	2.48	4.55	2.66
Rhizome/root	F	0.11	0.29	0.12	0.47	0.36	0.24	0.15	0.18	0.06	0.30	0.06
Rhizome/root	R	0.08	0.64	0.10	0.40	0.34	0.20	0.05	0.25	0.01	0.19	0.11
Rhizome/root	M	0.08	0.45	0.03	0.26	0.22	0.12	0.07	0.40	0.02	0.16	0.04
	average	0.09	0.46	0.08	0.38	0.31	0.19	0.09	0.28	0.03	0.22	0.07

Figure A.1: Principal Component Analysis of trace metal content in *Phragmites australis* plant compartments (L, leaves; S, stems; Rh, rhizomes; R, roots; and P, panicles) and sampling sites (F, Factory; R, Natural Reserve; M, Meander). Variance explained by PC1 = 54.5 %, PC2 = 14.0 %, and PC3 = 8.6 %.

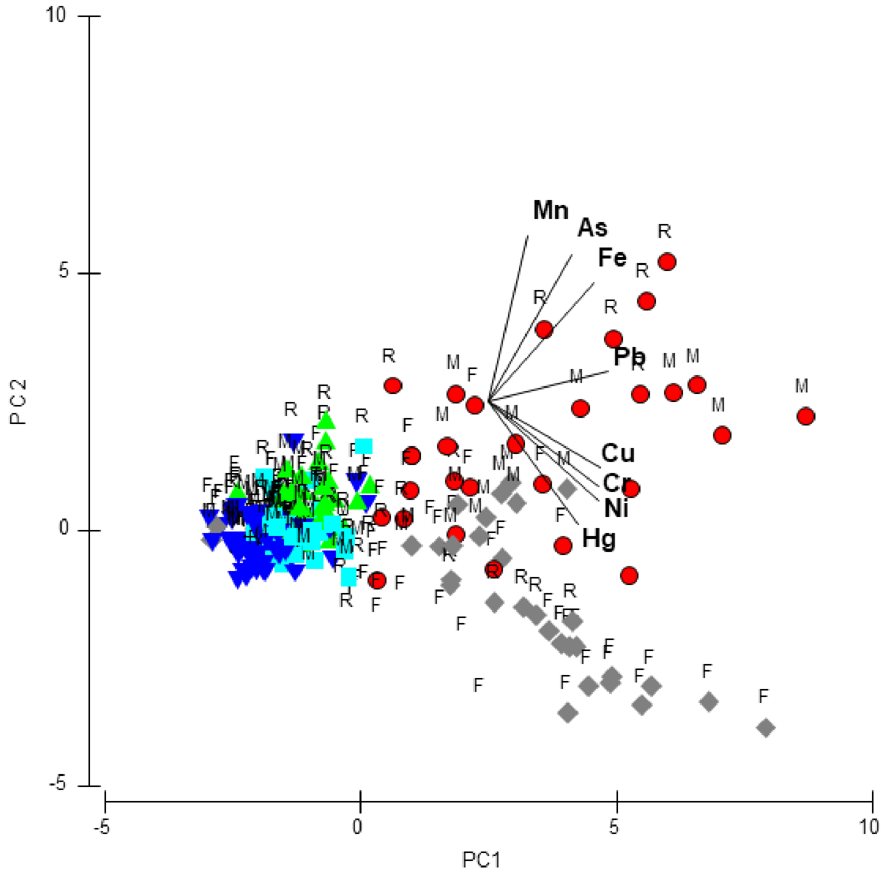

Figure A.2: Principal Component Analysis of trace metal concentrations *Phragmites australis* roots and panicles. Sampling sites: Factory (red dot), Natural Reserve (green square), and Meander (grey diamond).